

Boundary layer Viscous Flow of Nanofluids and Heat Transfer Over a Nonlinearly Isothermal Stretching Sheet in the Presence of Heat Generation/Absorption and Slip Boundary Conditions

Dodda Ramya^{1*}, R. Srinivasa Raju², J. Anand Rao¹ and M. M. Rashidi^{3,4}

¹Department of Mathematics, University College of Science, Osmania University, Hyderabad, 500007, Telangana State, India

²Department of Engineering Mathematics, GITAM University, Hyderabad Campus, Rudraram, 502329, Medak (Dt), Telangana State, India

³Shanghai Key Lab of Vehicle Aerodynamics and Vehicle Thermal Management Systems, Tongji University, 4800 Cao An Rd., Jiading, Shanghai 201804, China

⁴ENN-Tongji Clean Energy Institute of Advanced Studies, Shanghai, China

(*) Corresponding author: ramyadodda@gmail.com

(Received: 02 June 2016 and Accepted: 05 October 2016)

Abstract

The steady two-dimensional flow of a viscous nanofluid of magnetohydrodynamic (MHD) flow and heat transfer characteristics for the boundary layer flow over a nonlinear stretching sheet is considered. The flow is caused by a nonlinear stretching sheet with effects of velocity, temperature and concentration slips. Problem formulation is developed in the presence of heat generation/absorption and suction/injection parameters on non-linear stretching sheet. The resulting governing equations are converted into a system of nonlinear ordinary differential equations by applying a suitable similarity transformation and then solved numerically using Keller-Box technique. Convergences of the derived solutions are studied. The effects of the different parameters on the velocity, temperature, and concentration profiles are shown and discussed. Numerical values of local skin-friction coefficient, local Nusselt number and Sherwood number are tabulated. It is found that the velocity profiles decreases, temperature and concentration profiles increases with increasing of velocity slip parameter, and the thermal boundary layer thickness increases with increasing of Brownian motion and thermophoresis parameters.

Keywords: Nanofluid, MHD, Slip effects, Heat generation/absorption, Suction/Injection.

1. INTRODUCTION

The study of boundary layer viscous fluid flows and heat transfer due to stretching surface have many important applications in engineering process and industrial areas, such as materials manufactured by polymer extrusion, paper production and glass fiber, crystal growing, wire drawing and hot rolling, annealing and tinning of copper wires, stretching of plastic film, cooling of

electronic chips or metallic sheets, artificial fibers and many others. In all these cases, the final product of desired properties depends on the rate of cooling in the process and the process of stretching. Sakiadis [1] analyzed boundary-layer behavior on continuous solid surface; various aspects of the problem have been investigated by many authors. Gupta and Gupta [2] analyzed heat and mass transfer

on a stretching sheet with suction blowing. Sheikholeslami et al. [3] investigated forced convection heat transfer in a semi-annulus under the influence of a variable magnetic field. Cortell [4] investigated numerical analysis for flow and heat transfer in a viscous fluid over a nonlinearly stretching sheet problem in two different ways. Rashidi et al. [5] derived the governing equations of mixed convective heat transfer for MHD viscoelastic fluid flow with thermal radiation over a porous wedge. Sheikholeslami et al. [6] studied the free convection of magnetic nanofluid by considering MFD viscosity effect.

Nanofluid is described as a fluid containing nanometer-sized particles, called nanoparticles within the length scale of 1-100 nm diameter and 5% volume fraction of nanoparticles. These fluids are suspended in engineering colloidal system of nanoparticles in a base fluid. As oil, ethylene glycol and water are poor heat transfer fluids, because they have low thermal conductivities or low heat transfer properties. The nanoparticles can be used in metals such as (*Ag*, *Cu*), oxides (Al_2O_3), nitrides (*AlN*, *SiN*), carbides (*SiC*) or nonmetals (graphite, carbon nano-tubes). Nanotechnology has been widely used in heat transfer including microelectronics, pharmaceutical processes, fuel cells and hybrid-powered engines. Nanofluid term was first introduced by Choi [7]. Sheikholeslami et al. [8] investigated effect of electric field on hydrothermal behavior of nanofluid in a complex geometry. Makinde and Aziz [9], Bhattacharyya and Layek [10], Ibrahim et al. [11], Bachok et al. [12] studied the boundary layer problems of stagnation point flow over a stretching or shrinking sheet. Sheikholeslami and Rashidi [13], Sheikholeslami and Ganji [14] and Sheikholeslami and Ganji [15] were investigated heat transfer effects on nanofluids and in presence of magnetic field. Hamad et al. [16] investigated the magnetic field effects on free convection

flow of past a vertical semi-infinite flat plate of a nanofluid. In the similar analysis Sheikholeslami et al. [17] investigated heat transfer on Al_2O_3 water nanofluid flows in a semi annulus enclosure using Lattice Boltzmann method. Rashidi et al. [18] analyzed the buoyancy effect on MHD flow over a stretching sheet of a nanofluid in the effect of thermal radiation using RK iteration scheme. Abolbashari et al. [19] investigated on entropy analysis for an unsteady magnetohydrodynamic flow past a stretching permeable surface in nanofluid. Sheikholeslami et al. [20] solved the problem for MHD natural convection heat transfer of nanofluids using Lattice Boltzmann method. In a similar way, Sheikholeslami and Ganji ([21] and [22]) studied the heat and mass transfer problems with nanofluids. Sheikholeslami et al. [23] studied nanofluid flow and heat transfer over a stretching porous cylinder considering thermal radiation. Sheikholeslami [24] studied hydrothermal behavior of nanofluid fluid between two parallel plates. In this work, one of the plates was externally heated, and the other plate, through which coolant fluid was injected, expands or contracts with time. Ferrofluid flow and heat transfer in the presence of an external variable magnetic field was studied by Sheikholeslami [25] using the control volume based finite element method. Control volume-based finite element method was applied by Sheikholeslami and Rashidi [26] for simulating Fe_3O_4 -water nanofluid mixed convection heat transfer in a lid-driven semi annulus in the presence of a non-uniform magnetic field. Sheikholeslami et al. [27] studied the influence of non-uniform magnetic field on forced convection heat transfer of Fe_3O_4 -Water nanofluid. Sabbaghi and Mehravar [28] studied the enhancement of thermal performance of a micro channel heat sink by using nanoencapsulated phase change material (NEPCM) slurry as a cooling fluid instead of pure fluid. Kasaeian and Nasiri

[29] discussed the effects of adding nanoparticles including TiO_2 to a fluid media for purpose of free convection heat transfer improvement by assuming the free convection to be in laminar flow regime and the solutions and calculations were all done by the integral method. Sheikholeslami et al. [30] applied Homotopy perturbation method to investigate the effect of magnetic field on Cu -water nanofluid flow in non-parallel walls.

However, the previous studies have not considered combination of velocity, thermal, and mass slip effects, which are important in chemical engineering operations and materials processing. Many researchers have investigated in recent years on slip phenomena at the nanoscale and microscale, owing to potential applications in micro electromechanical systems and nano electromechanical systems related with the inclusion of velocity slip, temperature slip, and mass slip. Swati Mukhopadhyay [31] analyzed the boundary layer flow over a nonlinear stretching sheet through the porous with slip boundary conditions using shooting technique. Convective nanofluids flow of stretching sheet or shrinking sheet with thermal and solutal boundary conditions was studied by Uddin et al. [32], Kai-Long Hsiao [33] investigated stagnation electrical MHD nanofluids in mixed convection with slip boundary on a stretching sheet. Slip effects motion of peristaltic and nanofluids in a channel with wall properties were investigated by Mustafa et al. [34]. Sheikholeslami et al. [35] studied numerical investigation of magnetic nanofluid forced convective heat transfer in existence of variable magnetic field using two phase model. Sahoo [36] considered the heat transfer of a non-Newtonian fluid flows over a stretching sheet with partial slip. Noghrehabadi et al. [37] derived the problem over a stretching sheet prescribed constant wall temperature at the slip boundary conditions. Rashidi et al. [38] studied the steady MHD

convective and slip flow due to a rotating disk with Ohmic heating and viscous dissipation. Dhanai et al. [39] investigated the MHD mixed convection heat transfer and nanofluid flow over an inclined cylinder due to velocity and thermal slip effects by using Buongiorno's model. Sheikholeslami et al. [40] derived entropy generation of nanofluid in presence of magnetic field using Lattice Boltzmann Method.

The analysis of heat generation or absorption parameter effects on moving fluid is an important in view of several physical problems. Because of the fast growth of electronic technology, effective cooling of electronic equipment has become cooling of electronic equipment ranges and warranted from individual transistors to mainframe computers and from energy suppliers to telephone switch boards. By considering temperature dependent heat generation/absorption, several authors have investigated the heat transfer problems. But in recent applications, non-uniform heat generation plays a crucial role in heat transfer problems. Chamkha and Aly [41] considered MHD free convection of a nanofluid flow in the presence of heat source or sink effects past a vertical plate. In the similar way, Kandaswamy et al. [42] investigated the effects of, thermal stratification, chemical reaction and heat source on heat transfer problem. Rana and Bhargava [43] examined mixed convection flow of nanofluids with heat source or sink along a vertical plate using numerical technique Finite element method. Nandy and Mahapatra [44] analyzed the stagnation point flow of nanofluids over a stretching sheet or shrinking sheet with effects of slips and heat generation/absorption. The problem of carbon nanotubes suspended magneto hydrodynamic stagnation point flow over a stretching sheet for variable thermal conductivity with thermal radiation was studied numerically by Akbar et al. [45] using shooting technique. Uddin et al. [46]

studied two dimensional steady state laminar boundary layer flow of a viscous electrically-conducting nanofluid in the vicinity of a stretching/shrinking porous flat plate located in a Darcian porous medium using a variational finite element method. Ibrahim and Makinde [47] studied the effect of slip and convective boundary condition on magnetohydrodynamic stagnation point flow and heat transfer due to Casson nanofluid past a stretching sheet using the Runge-Kutta-Fehlberg method along with shooting technique. Abbas et al. [48] discussed the flow and heat transfer in a two-dimensional boundary layer flow of an electrically conducting nanofluid over a curved stretching sheet coiled in a circle of radius using shooting method. Anjali Devi and Suriyakumar [49] studied the steady two-dimensional mixed convective boundary layer flow of nanofluid over an inclined stretching plate with the effects of magnetic field, slip boundary conditions, suction and internal heat absorption. The analysis of mass transfer in two dimensional magnetohydrodynamic slip flow of an incompressible, electrically conducting, viscous and steady flow of alumina water nanofluid in the presence of magnetic field over a flat plate discussed by Singh and Kumar [50] using adaptive Runge-Kutta method with shooting technique. Hayat et al. [51] investigated MHD steady flow of viscous nanofluid due to a rotating disk using HAM solutions. Kiran Kumar et al. [52] studied unsteady MHD free convection flow of nanofluids through a porous medium bounded by a moving vertical semi-infinite permeable flat plate with constant heat source through porous medium. Das et al. [53] studied magnetohydrodynamics boundary layer slip flow over a vertical stretching sheet in nanofluid with non-uniform heat generation/absorption in the presence of a uniform transverse magnetic field using the Runge-Kutta fourth order method with shooting technique. The problem of magnetohydrodynamics boundary layer flow and heat transfer on a permeable

stretching surface in a nanofluid under the effect of heat generation and partial slip was simulated by Bhargava et al. [54] using variational finite element method as well as hybrid approach.

Transpiration of a fluid through the bounding surface can significantly change the flow field. In general, suction tends to enhance the skin friction whereas injection acts in the opposite manner. Injection or withdrawal of fluid through a porous bounding wall is of general interest in practical problems involving boundary layer control applications such as polymer fiber coating, film cooling and coating of wires. The process of suction and blowing has also its grandness in many engineering activities such as in the design of thrust bearing and radial diffusers, and thermal oil recovery. Suction is applied to chemical processes to remove reactants. Blowing is used to add reactants, cool the surface, prevent corrosion or scaling and reduce the drag. MHD boundary layer flow and heat transfer of a nanofluid past a permeable stretching sheet with velocity, thermal and solutal slip boundary conditions is studied by Ibrahim and Shankar [55]. Rashidi et al. [56] investigated on nanofluid dynamics from nonlinear isothermal stretching sheet with transpiration using Homotopy analysis method. Hamad and Ferdows [57] derived the problem on stagnation point flow of nanofluids effect of suction/blowing and heat generation/absorption through a heated porous stretching sheet using Lie group analysis. Sultana et al. [58] observed the heat transfer problem on stretching sheet effects of internal heat generation and suction or injection in presence of radiation using Nachtsheim-Swigert shooting iteration technique.

In the present study, we investigate the flow and heat transfer phenomena over a nonlinearly stretching sheet with the velocity, thermal and concentration slips effects at the boundary conditions. In addition, we added the heat source parameter in energy equation and suction

parameter at wall. This problem is extended to previous work done by Mabood et al. [59] and good agreement for four decimal places. The problem is solved by the Keller-box method. The effects of different flow parameters on the velocity, temperature, and concentration profiles were sketched and analyzed. In addition, the local skin-friction, the heat and mass transfer rates were examined.

2. MATHEMATICAL ANALYSIS

Let us consider the steady two-dimensional viscous flow of a nanofluid towards a nonlinear stretching surface with a linear velocity variation with the distance x , i.e. $u_w = ax^n$. Where a is a constant and n is a nonlinear stretching parameter. The nanofluid flows at $y \geq 0$, where y is the coordinate normal to the surface. The wall temperature T_w and the nanoparticle concentration fraction C_w are assumed constant at the stretching surface. When y tends to infinity; the ambient values of temperature and nanoparticle concentration fraction are denoted by T_∞ and C_∞ respectively. The fluid is electrically conducted due to an applied magnetic field normal to the stretching sheet. The magnetic Reynolds number is adopted small and so, the induced magnetic field $B(x)$ can be considered to be negligible. The coordinate system and the flow model are shown in Fig. 1.

Under the above assumptions, the governing equation of the conservation of mass, momentum, energy and nanoparticles fraction in the presence of heat source parameter, slip boundary conditions and suction parameter over a nonlinear stretching sheet can be written in cartesian coordinates x and y as (Khan and Pop [60], Goyal and Bhargava [61]):

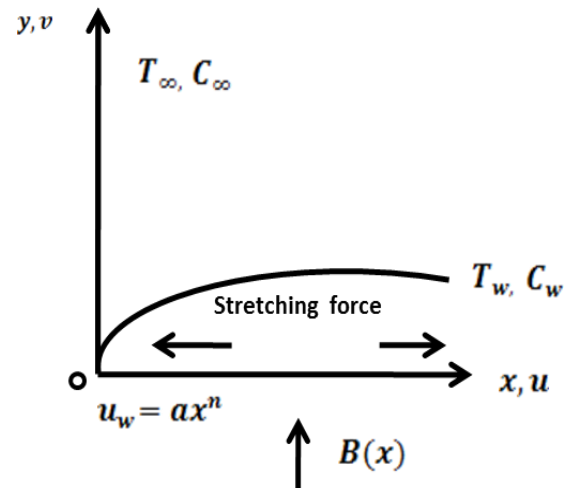


Figure 1. Physical model and coordinate system.

$$\frac{\partial u}{\partial x} + \frac{\partial v}{\partial y} = 0 \quad (1)$$

$$u \frac{\partial u}{\partial x} + v \frac{\partial u}{\partial y} = \nu \frac{\partial^2 u}{\partial y^2} - \frac{\sigma B^2(x)}{\rho_f} u \quad (2)$$

$$u \frac{\partial T}{\partial x} + v \frac{\partial T}{\partial y} = \alpha \frac{\partial^2 T}{\partial y^2} + \tau \left\{ D_B \frac{\partial C}{\partial y} \frac{\partial T}{\partial y} + \frac{D_T}{T_\infty} \times \left(\frac{\partial T}{\partial y} \right)^2 \right\} + \frac{v}{c_p} \left(\frac{\partial u}{\partial y} \right)^2 + \frac{Q_0}{(\rho c)_f} (T - T_\infty) \quad (3)$$

$$u \frac{\partial C}{\partial x} + v \frac{\partial C}{\partial y} = D_B \frac{\partial^2 C}{\partial y^2} + \left(\frac{D_T}{T_\infty} \right) \frac{\partial^2 T}{\partial y^2} \quad (4)$$

where $\alpha = \frac{K}{(\rho c)_f}$ is the thermal diffusivity

and $\tau = \frac{(\rho c)_p}{(\rho c)_f}$ is the ratio between the

effective heat capacity of the fluid. We assume that the variable magnetic field $B(x) = B_0 x^{n-1/2}$. This form of $B(x)$ has also been considered by Ishak [62] in their MHD flow problems. The boundary conditions for this problem are

$$u = u_w + K_1 \frac{\partial u}{\partial y}, \quad v = V_w, \quad T = T_w + K_2 \frac{\partial T}{\partial y}, \quad C = C_w + K_3 \frac{\partial C}{\partial y} \quad \text{at } y = 0, \quad (5)$$

$$u \rightarrow u_\infty, \quad T \rightarrow T_\infty, \quad C \rightarrow C_\infty \quad \text{as } y \rightarrow \infty$$

where $u_w = ax^n$, K_1 is the velocity slip parameter, K_2 is the thermal slip parameter, K_3 is the concentration slip parameter. Where V_w is the variable velocity components in vertical direction at

the stretching surface in which $V_w < 0$ represents to the suction cases and $V_w > 0$ represents to the injection ones.

Now we introducing similarity transformations

$$\begin{aligned} u &= ax^n f'(\eta), \\ v &= -\sqrt{\frac{av(n+1)}{2}} x^{\frac{n-1}{2}} \left(f(\eta) + \frac{n-1}{n+1} \eta f'(\eta) \right), \\ \eta &= y \sqrt{a(n+1)/2\nu_f} x^{(n-1)/2}, \\ \theta(\eta) &= \frac{T - T_\infty}{T_w - T_\infty} \end{aligned} \quad (6)$$

Substitute these transformations into the governing Eqs. (1)- (4), yields the reduced form of the conservation equations for momentum, energy and concentration.

$$f'''' + ff'' - \left(\frac{2n}{n+1}\right) f'^2 - Mf' = 0 \quad (7)$$

$$\frac{1}{Pr} \theta'' + f\theta' - \left(\frac{4n}{n+1}\right) f' \theta + Nb \theta' \phi' + Nt \theta^2 \quad (8)$$

$$\begin{aligned} + Ecf''^2 - Q\theta &= 0 \\ \phi'' + Lef\phi' + \frac{Nt}{Nb} \theta'' &= 0 \end{aligned} \quad (9)$$

The transformed conditions are

$$\begin{aligned} f' &= 1 + \lambda f''(0), f = S, \theta = 1 + \delta \theta'(0), \\ \phi &= 1 + \gamma \phi'(0) \text{ at } \eta = 0, \\ f' &\rightarrow 0, \theta \rightarrow 0, \phi \rightarrow 0 \text{ as } \eta \rightarrow \infty \end{aligned} \quad (10)$$

$$\begin{aligned} \text{Where } Pr &= \frac{\nu}{\alpha}, M = \frac{2\sigma B_0^2}{a\rho_f(n+1)}, \\ Le &= \frac{\alpha}{D_B}, Nb = \frac{(\rho c)_f D_B (C_w - C_\infty)}{(\rho c)_f \nu}, \\ Nt &= \frac{(\rho c)_f D_T (T_w - T_\infty)}{(\rho c)_f T_\infty \nu}, \lambda = \\ K_1 &\sqrt{\frac{av(n+1)}{2}} x^{n-\frac{1}{2}}, \\ \delta &= K_2 \sqrt{\frac{av(n+1)}{2}} x^{n-\frac{1}{2}}, \gamma = \\ K_3 &\sqrt{\frac{av(n+1)}{2}} x^{n-\frac{1}{2}}, Ec = \frac{u_w^2}{c_p(T_w - T_\infty)}, \\ S &= -V_w / \sqrt{\frac{av(n+1)}{2}} x^{n-1/2}, \\ Q &= \frac{2Q_0}{(\rho c)_f a(n+1)} x^{n-1/2} \end{aligned} \quad (11)$$

The quantities of the practical interest, in this study, are the local skin friction

$$\begin{aligned} C_{fx} &= \frac{\mu_f}{\rho u_w^2} \left[\frac{\partial u}{\partial y} \right]_{y=0}, Nu_x = \frac{x q_w}{k(T_w - T_\infty)}, \\ Sh_x &= \frac{x q_m}{D_B(C_w - C_\infty)} \end{aligned} \quad (12)$$

where k is the thermal conductivity of the nanofluid, and q_w, q_m are the heat and mass fluxes at the surface, given by

$$q_w = - \left[\frac{\partial T}{\partial y} \right]_{y=0}, q_m = -D_B \left[\frac{\partial C}{\partial y} \right]_{y=0} \quad (13)$$

Substituting Eq. (9) into Eqs. (11)- (13), we obtain

$$\begin{aligned} Re_x^{1/2} C_{fx} &= \sqrt{\frac{n+1}{2}} f''(0), \\ Re_x^{-1/2} Nu_x &= -\sqrt{\frac{n+1}{2}} \theta'(0), \\ Re_x^{1/2} Sh_x &= -\sqrt{\frac{n+1}{2}} \phi'(0) \end{aligned} \quad (14)$$

where $Re_x = u_w x / \nu$ is the local Reynolds number. This form of has also been considered by Mabood et al. [59] and Hamad et al. [63] in their MHD flow of nonlinear stretching sheet problems.

3. NUMERICAL SOLUTIONS BY KELLER-BOX METHOD

As Eqs. (7)-(9) are nonlinear, it is impossible to get the closed form solutions. Consequently, the equations with the boundary conditions (10) are solved numerically by means of a finite-difference scheme known as the Keller-box method. The principal steps in the Keller-box method to get the numerical solutions are the following:

- i). Reduce the given ODEs to a system of first order equations.
- ii). Write the reduced ODEs to finite differences.
- iii). Linearized the algebraic equations by using Newton's method and write them in vector form.
- iv). Solve the linear system by the block tridiagonal elimination technique.

One of the factors that are affecting the accuracy of the method is the appropriateness of the initial guesses. The accuracy of the method depends on the choice of the initial guesses. The choices of the initial guesses depend on the convergence criteria and the boundary conditions (14). The following initial guesses are chosen

$$\begin{aligned} f_0(\eta) &= S + (1/1 + \lambda) - (1/1 + \lambda)e^{-\eta}, \\ g_0(\eta) &= (1/1 + \delta)e^{-\eta}, \\ h_0(\eta) &= (1/1 + \gamma)e^{-\eta} \end{aligned} \quad (15)$$

In this study, a uniform grid of size $\Delta\eta = 0.006$ is found to satisfy the convergence and the solutions are obtained with an error of tolerance 10^{-5} in all cases. In our study, this gives about four decimal places accurate to most of the prescribed quantities.

4. RESULTS AND DISCUSSIONS

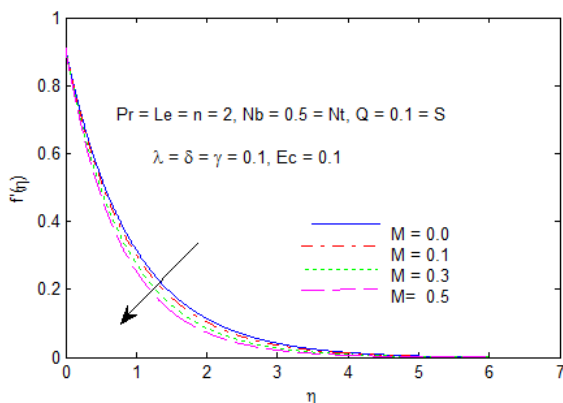


Figure 2. Effects of M on velocity profiles.

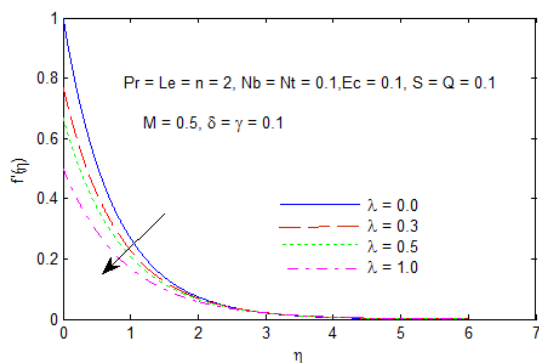


Figure 3. Effects of λ on velocity profiles.

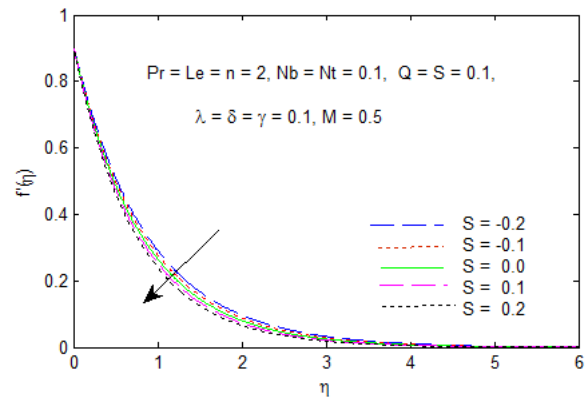


Figure 4. Effects of S on Velocity profiles.

In this section we present a comprehensive numerical parametric study is conducted and the results are reported graphically and in tabular form. Numerical simulations were carried out to obtain approximate numerical values of the quantities of engineering interest. The quantities are the skin-friction $f''(0)$, heat transfer rate $\theta'(0)$ and mass transfer rate $\phi'(0)$.

4.1. VELOCITY PROFILES

Figs. 2-4 shows that the velocity profiles for different values of the magnetic parameter (M), Suction (S) and Velocity slip (λ) parameters. Fig. 2 depicts the effect of Magnetic parameter on the dimensionless velocity. It is found that the increase of magnetic parameter decreases the velocity. The momentum boundary layer thickness is decreases with increasing values of M . The reason behind this aspect is that application of magnetic field to an electrically conducting fluid gives to a resistive type force called the Lorentz force which opposes the fluid motion. Fig. 3 depicts that the effect of velocity slip parameter λ on the dimensionless velocity. As velocity slip parameter λ increases then there is a decrement in velocity profile. It is observed that slip velocity is increases and consequently fluid velocity diminished because of the slip condition at the boundary. The pulling of the stretching sheet can only partly be transmitted to the

fluid. It is found that velocity slip λ has a substantial effect on the solutions.

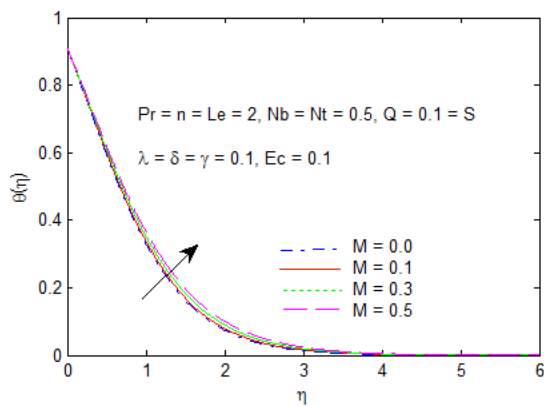


Figure 5. Effects of M on temperature profiles.

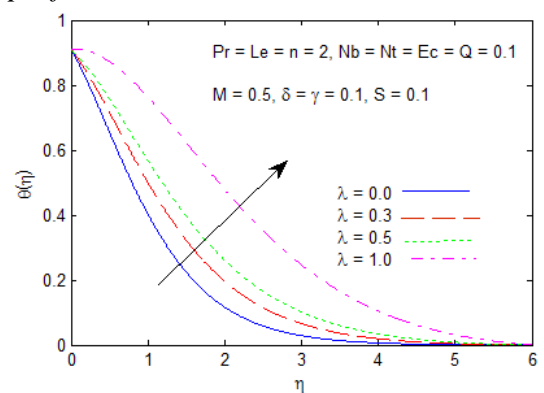


Figure 6. Effects of λ on temperature profiles.

Fig. 4 shows the effect of Suction blowing parameter S on velocity profile in presence of slip boundary conditions for non-linear stretching sheet. It is observed that the increasing suction parameter S , whereas fluid velocity is found to be increase with blowing in Fig. 4. It is found that, when the wall suction ($S > 0$) is considered, this causes a decrease in the boundary layer thickness and the dimensionless velocity field reduces. $S = 0$ represents the case of non-porous stretching sheet.

4. 2. TEMPERATURE PROFILES

Fig. 5 exhibits the effect of Magnetic parameter M on the dimensionless temperature profile. It is observed that the temperature profiles is increased with increase of Magnetic parameter M . The reason behind the increasing of the temperature on the

boundary layer is due to the fact that a body force (Lorentz force) is produced which opposes the fluid motion in the presence of transverse magnetic field and the resistance offers to the fluid flow which is responsible for the increase in the fluid temperature. By controlling the strength of the applied magnetic field, the surface temperature of the sheet can be controlled. Fig. 6 shows that the effects of velocity slip parameter λ on the temperature profiles. For the variation of velocity slip parameter λ in presence of suction. With the increasing λ , the temperature is found to be decreased initially but after a certain distance from the sheet it increases with slip parameter λ .

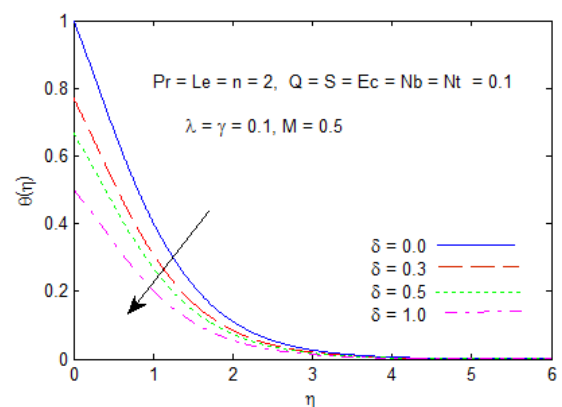


Figure 7. Effects of δ on temperature Profiles.

The influence of thermal slip parameter δ on dimensionless temperature is shown in Fig. 7. It is observed that as thermal slip parameter δ increases then the dimensionless temperature is decreases. It is found that initially the temperature reduces with thermal slip parameter δ but after a certain distance increases from the sheet, such feature is blurred out. With the increase of thermal slip parameter δ , less heat is transferred to the fluid from the sheet and so temperature is found to decreases. The influence of heat generation/ absorption parameter Q on the dimensionless temperature profiles are shown in Fig. 8. Here we observed that when the Heat generation/absorption parameter Q increases then the dimensionless temperature increased.

Increasing the heat generation parameter Q has the tendency to increase the thermal state of the fluid. This increase in the temperature fluid causes more induced flow towards the plate through the thermal buoyancy effect.

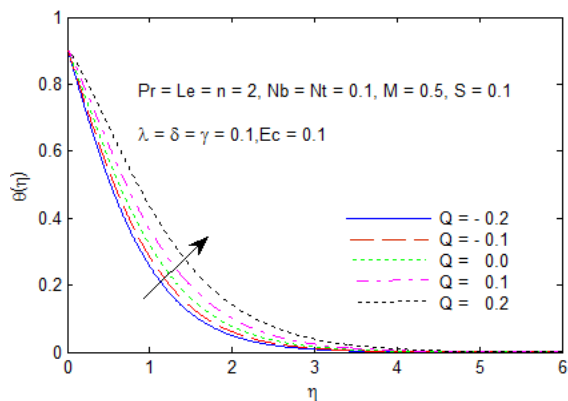


Figure 8. Effects of Q on temperature profiles

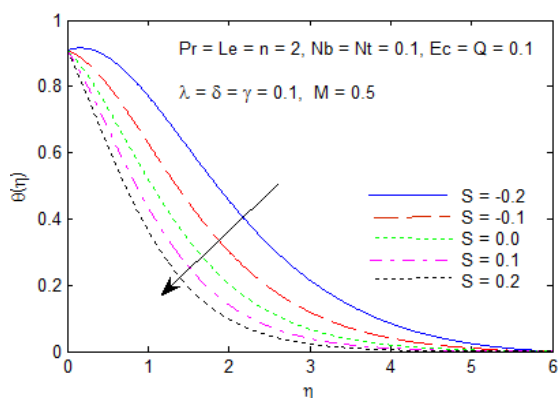


Figure 9. Effects of S on temperature profiles.

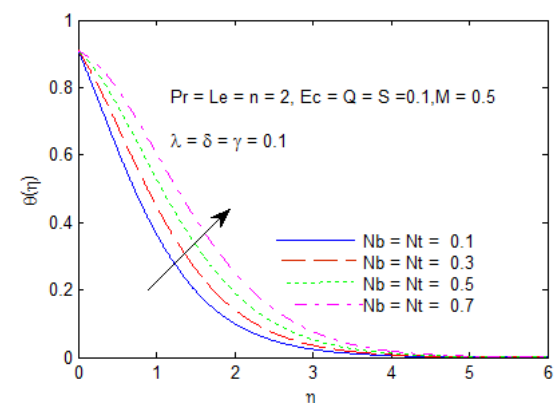


Figure 10. Effects of Nb, Nt on temperature profiles.

From Fig. 9, it is seen that temperature decreases with increasing suction

parameter whereas it increases due to blowing. Temperature wave-off is noted for suction blowing ($S < 0$). This feature prevails up to certain heights and then the process is decelerates and at a far distance from the wall temperature vanishes. Fig. 10 shows the effect of the Thermophoresis parameter Nt and Brownian motion parameter Nb on temperature distribution. As the parameters Nt and Nb increases, at a point the temperature increases. As a consequence, the thickness of the thermal boundary layer increases with the increase of Nt and Nb . This is because of the thermophoretic force generated by the temperature gradient creates a fast flow away from the stretching sheet. In this way more heated fluid is moved away from the stretching surface.

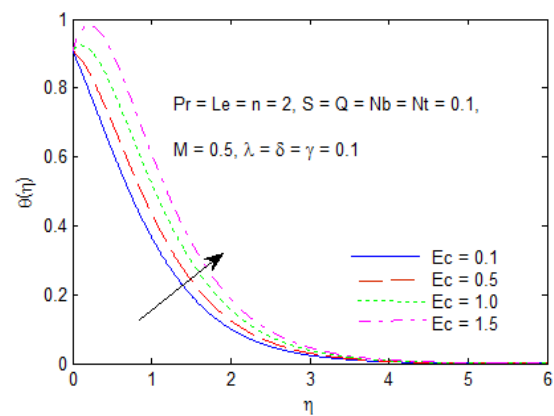


Figure 11. Effects of Ec on temperature profiles.

Fig. 11 depicts that the effect of viscous dissipation parameter Ec (Eckert number) on the dimensionless temperature. As the viscous dissipation parameter Ec increases then the dimensionless temperature also increases. Increasing the Eckert number allows energy to be stored in the fluid region as a result of profligacy due to viscosity and elastic deformation thus generating heat due to frictional heating. This is then causes the temperature within the fluid flow to greatly increase.

4. 3. CONCENTRATION PROFILES

Fig. 12 exhibits that the effect of Magnetic parameter M on the

dimensionless concentration profiles. It is observed that the concentration profile increases with increasing of Magnetic Parameter M . Fig. 13 depicts the effect of velocity slip parameter λ on the nanoparticle concentration. As the velocity slip parameter increases, the concentration profile also increases.

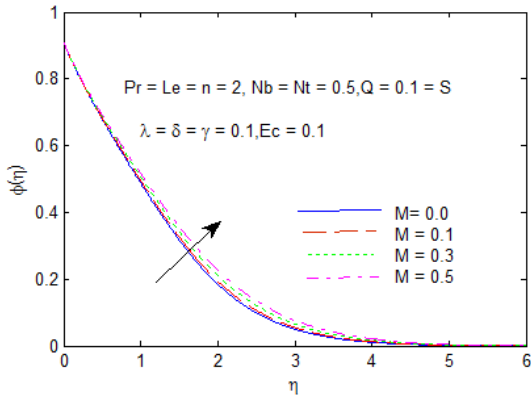


Figure 12. Effect of M on concentration profiles.

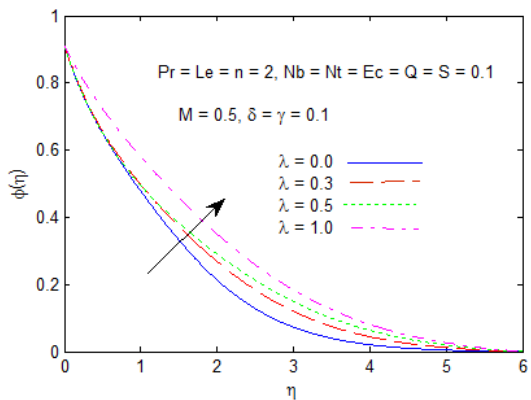


Figure 13. Effect of λ concentration profiles.

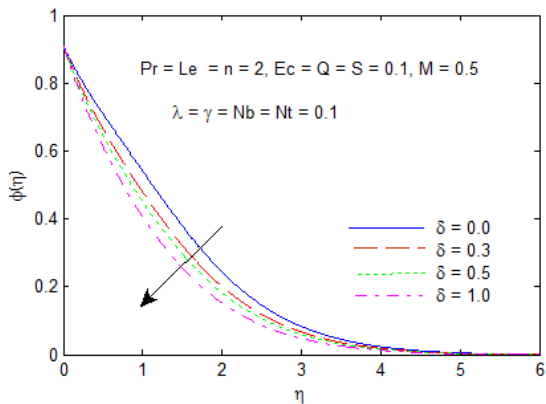


Figure 14. Effect of δ on concentration profiles.

Fig. 14 illustrates different values of thermal slip parameter δ for the stretching sheet. It is observed that the nanoparticle volume fraction increases with the increasing of thermal slip. Fig. 15 illustrates the variation of concentration with respect to concentration slip parameter γ . As it can be seen from the graph, the concentration profile reduces when Solutal slip parameter γ increases parameter δ .

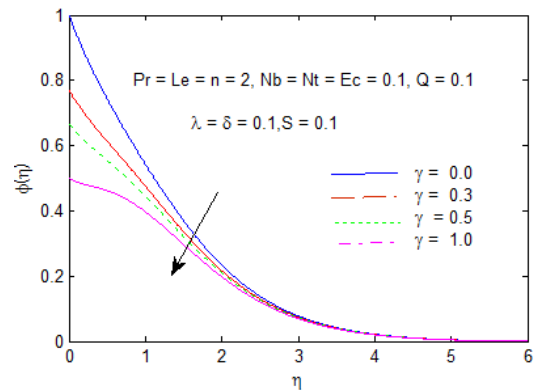


Figure 15. Effect of γ on concentration profiles.

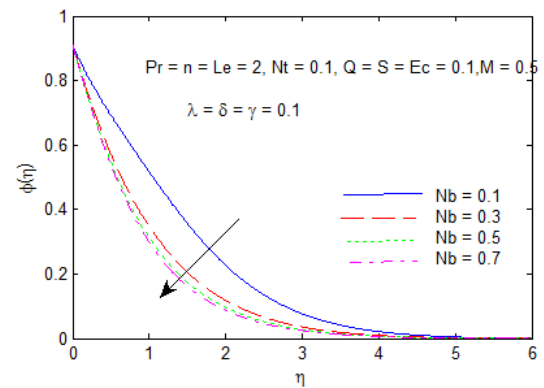


Figure 16. Effect of Nb on concentration profiles.

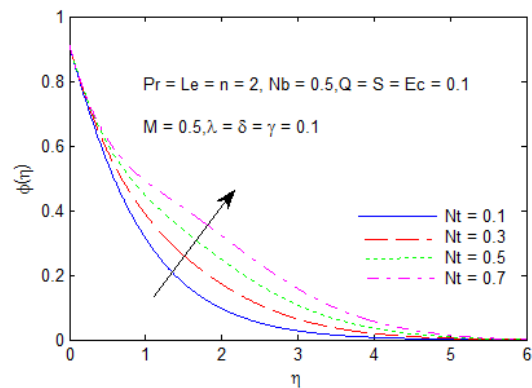


Figure 17. Effects of Nt on concentration profiles.

The influence of Brownian motion parameter Nb and thermophoresis parameter Nt on concentration profile are shown in Figs. 16 and 17. From these figures it can be observed that the concentration profiles is increases with increasing values of thermophoresis parameter Nt . As the Brownian motion parameter Nb of the fluid increases, it leads to a decreases in the concentration inside the boundary layer. Fig. 18 illustrates the effect of Lewis number Le on the nanoparticle volume fraction. As the Lewis number Le gains then reduces in the Concentration profiles. The larger values of Lewis number makes the smaller molecular diffusivity, therefore it decreases the concentration field.

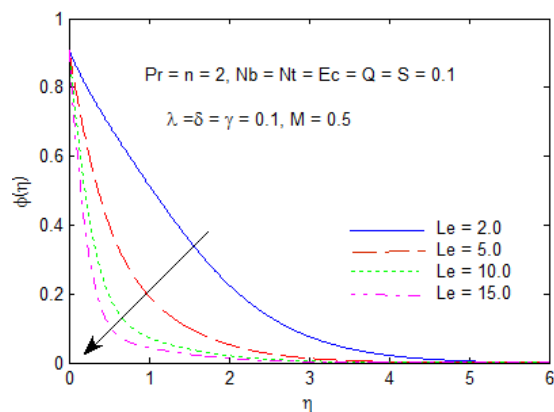


Figure 18. Effects of Le on concentration profiles.

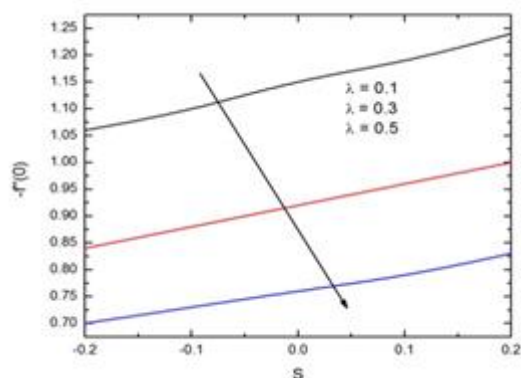


Figure 19. Effect of λ on skin-friction coefficient.

Figs. 19-23 illustrates the effect of skin-friction coefficient, local Nusselt number

and Sherwood numbers for various values of velocity slip parameter, thermal slip parameter and concentration slip parameter. Fig. 19 exhibits the nature of skin-friction coefficient ($-f''(0)$) with suction or injection parameter (S) for two values of velocity slip parameter (λ). It is found that decreases in the skin-friction coefficient with S whereas it increases with the higher values of slip velocity parameter at the boundary. Fig. 20 depicts the effect of nonlinear stretching parameter and magnetic field effects on local Nusselt number. It is observed that as increasing n and M values reduced the rate of heat transfer.

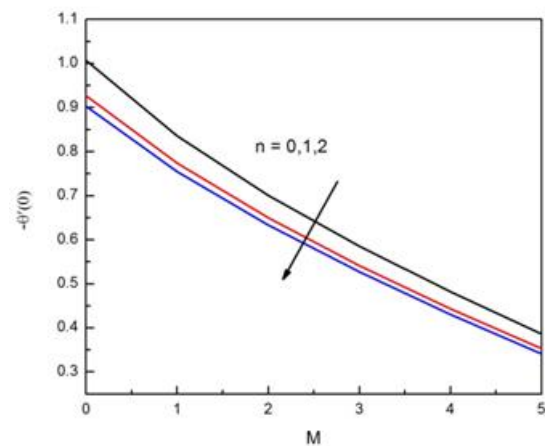


Figure 20. Effects of n on Nusselt number.

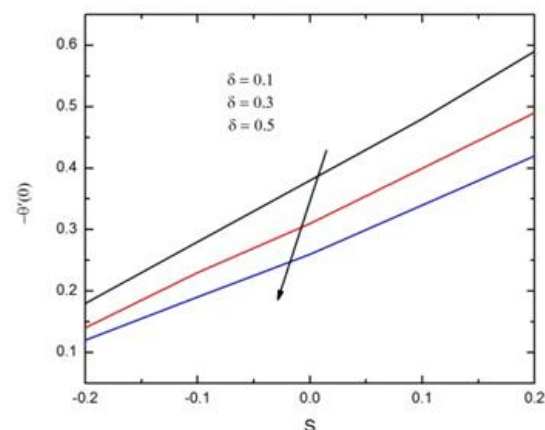


Figure 21. Effects of δ on Nusselt number.

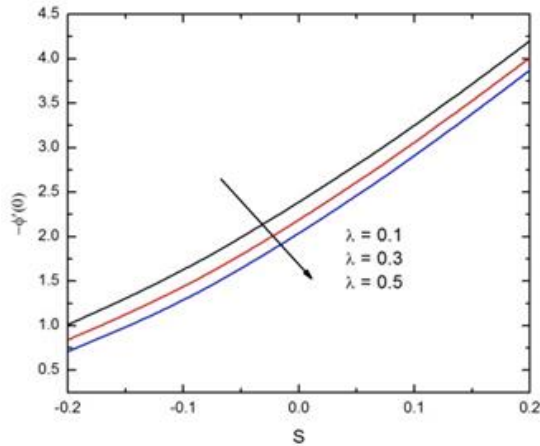


Figure 22. Effects of λ on Sherwood number.

Fig. 21 reveals the behavior of heat transfer coefficient ($-\theta'(0)$) with suction or injection parameter (S) for the values of thermal slip parameter δ . It is observed that as increasing thermal slip parameter values the heat transfer rate decreases. Fig. 22 presents the behavior of mass transfer coefficient ($-\phi'(0)$) with suction/injection parameter (S) for values of velocity slip parameter. It is very clear that mass

transfer decreases with increasing values of suction and also with increasing values of velocity slip. Fig. 23 shows the effect of concentration slip parameter (γ) on rate of mass transfer ($-\phi'(0)$). It is found that the mass transfer decreases with increasing concentration slip parameter (γ).

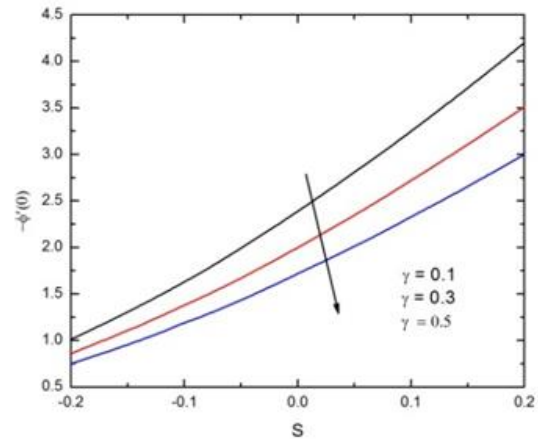


Figure 23. Effects of γ on Sherwood number.

Table 1. Comparison of $-\theta'(0)$ for Pr and n values when $Nb = Nt = S = Q = 0$

Pr	n	Cortell [4]	Zaimi et al. [64]	Mabood et al. [59]	Present results for different grid size (h)		
					$h = 0.1$	$h = 0.01$	$h = 0.006$
1	0.2	0.61026	0.61131	0.61131	0.6102	0.6102	0.6112
	0.5	0.59527	0.59668	0.59668	0.5952	0.5952	0.5966
	1.5	0.57453	0.57686	0.57686	0.5747	0.5747	0.5768
	3.0	0.56447	0.56719	0.56719	0.5647	0.5646	0.5671
	10.0	0.55496	0.55783	0.55783	0.5548	0.5549	0.5578
5	0.2	1.60717	1.60757	1.60757	1.6102	1.6077	1.6074
	0.5	1.58674	1.58658	1.58658	1.5890	1.5867	1.5864
	1.5	1.55746	1.55751	1.55751	1.5596	1.5576	1.5574
	3.0	1.54233	1.54271	1.54271	1.5450	1.5431	1.5429
	10.0	1.52857	1.52877	1.52877	1.5306	1.5288	1.5286

Table 2. Comparison of $-\theta'(0)$ and $-\phi'(0)$ for values when $Pr = Le = 2, M = EC = Q = S = 0$

			Rana & Bhargava [65] (FEM)	Malvandi et al. [66] (HAM)	Present study (Keller-Box Method)

n	Nt	Nb	$-\theta'(0)$	$-\phi'(0)$	$-\theta'(0)$	$-\phi'(0)$	$-\theta'(0)$	$-\phi'(0)$
0.2	0.1	0.5	0.5160	0.9012	0.5157	0.9003	0.51472	0.90094
		2.5	0.0303	0.9493	0.0302	0.9497	0.02988	0.94888
	0.3	0.5	0.4533	0.8395	0.4522	0.8406	0.4520	0.84024
		2.5	0.0265	0.9571	0.0263	0.9574	0.02609	0.95719
3	0.1	0.5	0.4864	0.8445	0.4854	0.8450	0.02609	0.84477

To validate the present solutions, comparisons have been made with previously published authors Mabood et al. [59], Cortell [4], Zaimi et al. [64], Rana and Bhargava [65], Malvandi et al. [66] and it is observed that good agreement for their results shows in Tables-1 and 3 for skin-friction, Nusselt number and Sherwood numbers. Tables-4 and 5 shows that effects of suction, heat generation, velocity slip, thermal slip and concentration slip parameters on skin-friction coefficient, Nusselt number and

Sherwood numbers. Clearly, it is observed that as increasing suction/injection parameter increases the skin-friction, rate of heat transfer and mass transfer rate. From Table-5, we observed that λ is increased then $-f''(0)$, $-\theta'(0)$ and $-\phi'(0)$ are decreased. With increasing the values of δ , the heat transfer rate decreases and the mass transfer rate increases. Finally as γ the rate of heat transfer increases and the rate of mass transfer decreases.

Table 3. For Comparison of skin-friction coefficient, Nusselt number and Sherwood number values when $Pr = 6.2$, $Le = 5$, $Nb = 0.1$, $Nt = 0.1$, $n = 2$, $\lambda, \delta, \gamma = 0$, and $s = 0$

Ec	M	$-f''(0)$		$-\theta'(0)$		$-\phi'(0)$	
		Mabood et al. [59]	Present Work	Mabood et al. [59]	Present Work	Mabood et al. [59]	Present Work
0	0	1.1010	1.10142	1.0671	1.06713	1.0771	1.07684
0.1				0.8819	0.88888	1.2234	1.22329
0.2				0.7099	0.70941	1.3707	1.37081
0.3				0.5295	0.52869	1.5191	1.51941
0.5				0.1648	0.16344	1.8193	1.81995
0	0.5	1.3098	1.30991	1.0436	1.04365	1.0100	1.0109
0.1				0.8105	0.81053	1.2060	1.20603
0.2				0.5756	0.57560	1.4027	1.40279
0.3				0.3388	0.33883	1.6011	1.60119
0.5				0.1402	0.14033	2.0028	2.00287
0.0	1	1.4891	1.48912	1.0233	1.02337	0.9549	0.95494
0.1				0.7405	0.74057	1.1949	1.19495
0.2				0.4554	0.45542	1.4370	1.43706
0.3				0.1678	0.16788	1.6812	1.68218
0.5				0.4145	0.41452	2.1762	2.17624

Table 4. Calculation table for $-f''(0)$, $-\theta'(0)$ and $-\phi'(0)$ when Suction/injection (S), heat generation/absorption (Q) parameters.

S	Q	$-f''(0)$	$-\theta'(0)$	$-\phi'(0)$
-0.2	0.0	1.06654	0.36485	0.35807
-0.1		1.10832	0.45524	0.38331
0.0		1.15191	0.55283	0.40697
0.1		1.19733	0.65673	0.42930
0.2		1.24457	0.76613	0.45055
0.1	-0.2	1.19733	0.86058	0.25433
	-0.1		0.76499	0.33683
	0.0		0.65673	0.42930
	0.1		0.52908	0.53690
	0.2		0.36681	0.67137

Table 5. Calculation of $-f''(0)$, $-\theta'(0)$ and $-\phi'(0)$ for various values of slip parameters λ , δ , γ when $Pr = n = Le = 2$, $Ec = Nb = Nt = Q = S = 0.1$

λ	δ	γ	$-f''(0)$	$-\theta'(0)$	$-\phi'(0)$
0.0	0.1	0.1	1.35981	0.54868	0.56903
0.1			1.19733	0.52908	0.53690
0.3			0.96024	0.48704	0.49330
0.5			0.79685	0.44542	0.46693
1.0			0.55170	0.35146	0.4404
1.0	0.0	0.1	1.19733	0.58661	0.50010
	0.1			0.52908	0.53690
	0.3			0.43902	0.59479
	0.5			0.37176	0.63822
	1.0			0.26023	0.71060
	1.0	0.0	1.19733	0.52238	0.62861
		0.1		0.52908	0.53690
		0.3		0.53949	0.39572
		0.5		0.54720	0.29211
		1.0		0.55986	0.12361

5. CONCLUSIONS

A numerical study of the boundary layer flow in a nanofluid over nonlinearly stretching sheet has been performed. A similarity solution is presented which depends on Lewis numbers, magnetic, viscous dissipation, Brownian motion and the thermophoresis parameters. The effects of governing parameters on the flow, concentration and heat transfer characteristics are presented graphically and quantitatively. The observations of the present study are as follows:

1. By increasing the values of Magnetic Parameter M and Velocity slip parameter λ on Velocity, Temperature and Concentration profiles then there is reduction in velocity profile and increase in the Temperature and Concentration profiles. This is due to the effect of Lorentz force.
2. When the Thermal Slip Parameter δ increases, then it reduces the temperature and concentration profiles.

3. Concentration profile is reduced when the Concentration Slip Parameter γ and Lewis number Le are increased.
4. Both Velocity profiles and the Temperature profiles are reduced by the increasing values of Suction/injunction S .
5. Temperature Profile is increased with the increasing values of Heat generation/absorption parameter Q .
6. By increasing the values of Brownian motion parameter Nb then the Temperature profiles is increased and Concentration profiles is decreased.
7. By increasing the values of Thermophoresis parameter Nt then the Temperature and Concentration profiles are increased.
8. Temperature profile is increased by the increase of Eckert number Ec .
9. The skin-friction coefficient and heat transfer rate decreases with increasing values of λ .
10. Rate of heat transfer decreases, whereas mass transfer rate decrease with thermal slip δ and concentration slip γ parameters.

NOMENCLATURE

List of variables

- u, v : Velocity components in the x - and y -axis, respectively (m/s)
- U_w : Velocity of the wall along the x -axis (m/s)
- x, y : Cartesian coordinates measured along the stretching sheet (m)
- $B(x)$: Magnetic field strength ($A m^{-1}$)
- C : Nanoparticle concentration ($mol m^{-3}$)
- C_{fx} : Skin-friction coefficient (*Pascal*)
- Nu_x : Nusselt number
- Sh_x : Sherwood number
- C_w : Nanoparticles concentration at the stretching surface ($mol m^{-3}$)
- C_∞ : Nanoparticle concentration far from the sheet ($mol m^{-3}$)
- C_p : Specific heat capacity at constant pressure ($J Kg^{-1} K$)
- D_T : Brownian diffusion coefficient

- D_B : Thermophoresis diffusion coefficient
- Ec : Eckert number
- a : Constant parameter
- n : Nonlinear stretching parameter
- f : Dimensionless stream function
- k : Thermal conductivity ($W m^{-1} K^{-1}$)
- S : Suction/injection parameter
- Le : Lewis number
- M : Magnetic parameter
- Q_0 : Dimensional heat generation parameter
- Nb : Brownian motion parameter
- Nt : Thermophoresis parameter
- Pr : Prandtl number
- Q : Heat generation/absorption parameter
- K_1 : Velocity slip factor
- K_2 : Thermal slip factor
- K_3 : Concentration slip factor
- T : Fluid temperature (K)
- q_w : Surface heat flux (W/m^2)
- T_w : Temperature at the surface (K)
- T_∞ : Temperature of the fluid far away from the stretching sheet (K)
- Re_x : Reynolds number
- q_m : Surface mass flux

Greek Symbols

- α : Thermal diffusivity (m^2/s)
- η : Dimensionless similarity variable
- μ : Dynamic viscosity of the base fluid ($kg/m.s$)
- ν : Kinematic viscosity ($m^2 s^{-1}$)
- ρ_f : Density of the fluid ($Kg m^{-3}$)
- ρ_p : Density of the nanoparticle ($Kg m^{-3}$)
- τ : The ratio of the nanoparticle heat capacity & the base fluid heat Capacity
- $(\rho c)_f$: Heat capacity of the base fluid ($kg/m.s^2$)
- $(\rho c)_p$: Heat capacity of the nanoparticle ($kg/m.s^2$)
- θ : Dimensionless temperature (K)
- p : pressure (N/m^2)
- ϕ : Nanoparticle volume fraction
- ϕ_w : Nanoparticle volume fraction at wall temperature

ϕ_{∞} : Ambient nanoparticle volume fraction

λ : Velocity slip parameter

δ : Thermal slip parameter

γ : Concentration slip parameter

Sub Scripts

f : Fluid

w : Condition on the sheet

∞ : Ambient Conditions

Superscripts

' : Differentiation w.r.t

ACKNOWLEDGEMENT

The authors thank the reviewers for their constructive suggestions and comments, which have improved the quality of the article considerably.

REFERENCES

1. Sakiadis B. C., (1961). "Boundary-layer behavior on continuous solid surface: I. Boundary-layer equations for two-dimensional and axisymmetric flow", *American Inst. Chemical Eng. J.*, 7: 26-28.
2. Gupta P. S., Gupta A. S., (1977). "Heat and Mass Transfer on a Stretching Sheet with Suction or Blowing", *The Canadian J. Chemical Eng.*, 55.
3. Sheikholeslami M., Vajravelu K., Rashidi M. M., (2016). "Forced convection heat transfer in a semi annulus under the influence of a variable magnetic field", *Int. J. Heat Mass Transf.*, 92: 339-348.
4. Cortell R., (2007). "Viscous flow and heat transfer over a nonlinearly stretching sheet", *Appl. Math. Computs*, 184: 864-873.
5. Rashidi M. M., Ali M., Freidoonimehr N., Rostami B., Hossain M. A., (2014). "Mixed convective heat transfer for MHD viscoelastic fluid flow over a porous wedge with thermal radiation", *Adv. Mech. Eng.*, 2014: 735939.
6. Sheikholeslami M., Rashidi M. M., Hayat T., Ganji, D. D., (2016). "Free convection of magnetic nanofluid considering MFD viscosity effect", *J. Molecular Liquids*, 218: 393-399.
7. Choi, S. U. S., (1995). "Enhancing thermal conductivity of fluids with nanoparticles, *ASME Int. Mech. Eng. Congress. San Francisco*, USA, ASME, FED, 231/MD., 66: 99-105.
8. Sheikholeslami M., Soleimani S., Ganji D. D., (2016). "Effect of electric field on hydrothermal behavior of nanofluid in a complex geometry", *J. Molecular Liquids*, 213: 153-161.
9. Makinde O. D., Aziz A., (2011). "Boundary layer flow of a nanofluid past a stretching sheet with a convective boundary condition", *Int. J. Thermal Sci.*, 50: 1326-1332.
10. Bhattacharyya K., Layek, G. C., (2011). "Effects of suction/blowing on steady boundary layer stagnation-point flow and heat transfer towards a shrinking sheet with thermal radiation", *Int. J. Heat Mass Transf.* 54: 302-307.
11. Ibrahim W., Shankar B., Mahantesh M., Nandeppanavar, (2013). "MHD stagnation point flow and heat transfer due to nanofluid towards a stretching sheet", *Int. J. Heat Mass Transf.*, 56: 1-9.
12. Bachok N., Ishak A., Pop I., (2011). "Stagnation-point flow over a stretching/shrinking sheet in a nanofluid", *Nanoscale Research Lett.*, 6: 623.
13. Sheikholeslami M., Rashidi M. M., (2015). "Effect of space dependent magnetic field on free convection of Fe_3O_4 -water nanofluid", *J. Taiwan Inst. Chemical Eng.*, 56: 6-15.
14. Sheikholeslami M., Ganji, D. D., (2014). "Ferrodynamics and magneto hydrodynamic effects on ferrofluid flow and convective heat transfer", *Energy*, 75: 400-410.
15. Sheikholeslami M., Ganji D. D., (2014). "Heated Permeable Stretching Surface in a Porous Medium Using Nanofluids", *J. Appl. Fluid Mech.*, 7: 535-542.
16. Hamad, M. A. A., Pop I., Ismail A. I. Md., (2011). "Magnetic field effects on free convection flow of a nanofluid past a vertical semi-infinite flat plate", *Nonlinear Anal. Real World Appl.*, 12: 1338-1346.
17. Sheikholeslami M., Gorji-Bandpy M., Ganji D. D., (2013). "Numerical investigation of MHD effects on Al_2O_3 -water nanofluid flow and heat transfer in a semi-annulus enclosure using LBM", *Energy*, 60: 501-510.
18. Rashidi M. M., Vishnu Ganesh N., Abdul Hakeem A. K., Ganga B., (2014). "Buoyancy effect on MHD flow of nanofluid over a stretching sheet in the presence of thermal radiation", *J. Molecular Liq.*, 198: 234-238.
19. Abolbashari M. H., Freidoonimehr N., Nazari F., Rashidi, M. M., (2014). "Entropy Analysis for an Unsteady MHD Flow past a Stretching Permeable Surface in Nano-Fluid", *Powder Technol.*, 267: 256-267.
20. Sheikholeslami M., Gorji-Bandpy M., Ganji, D. D., (2014). "Lattice Boltzmann method for MHD natural convection heat transfer using nanofluid", *Powder Technol.*, 254: 82-93.
21. Sheikholeslami M., Ganji D. D., (2013). "Heat transfer of Cu -Water nanofluid flow between parallel plates", *Powder Technol.*, 235: 873-879.

22. Sheikholeslami M., Ganji D. D., (2014). "Three dimensional hat and mass transfer in a rotating system using nanofluid", *Powder Technol.*, 253: 789-796.
23. Sheikholeslami M., Mustafa T., Ganji D. D., (2015). "Nanofluid flow and heat transfer over a stretching porous cylinder considering thermal radiation", *Iranian J. Sci. & Tech.*, 433-440.
24. Sheikholeslami M., (2014). "KKL correlation for simulation of nanofluid flow and heat transfer in a permeable channel", *Physics Lett. A*, 378: 3331-3339.
25. Sheikholeslami M., (2014). "Effect of spatially variable magnetic field on ferrofluid flow and heat transfer considering constant heat flux boundary condition", *The European Physical J. Plus*, 129: 248.
26. Sheikholeslami M., Rashidi M. M., (2015). "Ferrofluid heat transfer treatment in the presence of variable magnetic field", *The European Physical J. Plus*, 130: 115.
27. Sheikholeslami M., Rashidi M. M., Ganji D. D., (2015). "Effect of Non-uniform Magnetic Field on Forced Convection Heat Transfer of Fe_3O_4 -Water Nanofluid", *Comput. Methods Appl. Mech. Eng.*, 294: 299-312.
28. Sabbaghi, S., Mehravar, S., (2015). "Effect of Using Nano Encapsulated Phase Change Material on Thermal Performance of Micro Heat Sink", *Int. J. Nanosci. Nanotechnol.*, 11: 33-38.
29. Kasaean A. B., Nasiri Sh., (2015). "Convection Heat Transfer Modeling of Nano- fluid TiO_2 Using Different Viscosity Theories", *Int. J. Nanosci. Nanotechnol.*, 11: 45-51.
30. Sheikholeslami M., Mollabasi H., Ganji D. D., (2015). "Analytical Investigation of MHD Jeffery-Hamel Nanofluid Flow in Non-Parallel Walls", *Int. J. Nanosci. Nanotechnol.*, 11: 241-248.
31. Swati Mukhopadhyay, (2013). "Analysis boundary layer flow over a porous nonlinear stretching sheet with partial slip at the boundary", *Alexandria Eng. J.*, 52: 563-569.
32. Uddin Md. J., Bég O. A., Ismail A. I., (2015). "Radiative convective nanofluid flow past a stretching/shrinking sheet with slip effects", *J. Thermodynamics and Heat Transf.*, 29: 513-523.
33. Hsiao K. L., (2016). "Stagnation electrical MHD nanofluid mixed convection with slip boundary on a stretching sheet", *Appl. Thermal Eng.*, 98: 850-861.
34. Mustafa M., Hina S., Hayat T., Alsaedi A., (2013). "Slip effects on the peristaltic motion of nanofluid in a channel with wall properties", *J. Heat Transf.*, 135.
35. Sheikholeslami M., Rashidi M. M., Ganji, D. D., (2015). "Numerical investigation of magnetic nanofluid forced convective heat transfer in existence of variable magnetic field using two phase model", *J. Molecular Liq.*, 212: 117-126.
36. Sahoo B., (2010). "Flow and heat transfer of a non-Newtonian fluid past a stretching sheet with partial slip", *Commun. Nonlinear Sci. Numer. Simul.*, 15: 602-615.
37. Noghrehabadi A., Pourrajab R., Ghalambaz Md., (2012). "Effect of partial slip boundary condition on the flow and heat transfer of nanofluids past stretching sheet prescribed constant wall temperature", *Int. J. Thermal Sci.*, 54: 253-261.
38. Rashidi M. M., Erfani E., (2012). "Analytical Method for Solving Steady MHD Convective and Slip Flow due to a Rotating Disk with Viscous Dissipation and Ohmic Heating", *Eng. Comput.*, 29: 562-579.
39. Dhanai R., Rana P., Kumaar L., (2016). "MHD mixed convection nanofluid flow and heat transfer over an inclined cylinder due to velocity and thermal slip effects: Buongiorno's model", *Powder Technol.*, 288: 140-150.
40. Sheikholeslami M., Ganji D. D., (2015). "Entropy generation nanofluid in presence of magnetic field using Lattice Boltzman Method", *Physica A*, 417: 273-286.
41. Chamkha A. J., Aly A. M., (2010). "MHD free convection flow of a Nanofluid past a vertical plate in the presence of heat generation or absorption effects", *Chemical Eng. Commun.*, 198: 425-441.
42. Kandasamy R., Periasamy K., Sivagnana Prabhu K. K., (2005). "Chemical reaction, heat and mass transfer on MHD flow over a vertical stretching surface with heat source and thermal stratification effects", *Int. J. Heat Mass Transf.*, 48: 4557-4561.
43. Rana P., Bhargava R., (2011). "Numerical study of heat transfer enhancement in mixed convection flow along a vertical plate with heat source/sink utilizing nanofluids", *Commun. Nonlinear Sci. Numer. Simul.*, 16: 4318-4334.
44. Nandy S. K., Mahapatra T. R., (2013). "Effects of slip and heat generation/absorption on MHD stagnation point flow nanofluid past a stretching/shrinking surface with convective boundary conditions", *Int. J. Heat Mass Transf.*, 64: 1091-1100.
45. Akbar N. S., Khan Z. H., (2016). "Effect of variable thermal conductivity and thermal radiation with CNTS suspended nanofluid over a stretching sheet with convective slip boundary conditions: Numerical study", *J. Molecular Liq.*, 222: 279-286.
46. Uddin M. J., Rana P., Anwar Bég O., Ismail A. I. M., (2016). "Finite element simulation of magneto hydrodynamic convective nanofluid slip flow in porous media with nonlinear radiation", *Alexandria Eng. J.*, 55: 1305-1319.

47. Ibrahim W., Makinde O. D., (2016). "Magnetohydrodynamic Stagnation Point Flow and Heat Transfer of Casson Nanofluid Past a Stretching Sheet with Slip and Convective Boundary Condition", *J. Aerospace Eng.*, 29: 04015037.
48. Abbas Z., Naveed M., Sajid M., (2016). "Hydromagnetic slip flow of nanofluid over a curved stretching surface with heat generation and thermal radiation", *J. Molecular Liq.*, 215: 756-762.
49. Anjali Devi S. P., Suriyakumar P., (2016). "Hydromagnetic mixed convective nanofluid slip flow past an inclined stretching plate in the presence of internal heat absorption and suction", *J. Appl. Fluid Mech.*, 9: 1409-1419.
50. Singh P., Kumar M., (2015). "Mass transfer in MHD flow of alumina water nanofluid over a flat plate under slip conditions", *Alexandria Eng. J.*, 54: 383-387.
51. Hayat T., Rashid M., Imtiaz M., Alsaedi A., (2015). "Magneto hydrodynamic (MHD) flow of Cu-water nanofluid due to a rotating disk with partial slip", *AIP Advances*, 5: 067169.
52. Kiran Kumar R. V. M. S. S., Durga Prasad P., Varma S. V. K., (2015). "Analytical Study of Heat and Mass Transfer Enhancement in Free Convection Flow with Chemical Reaction and Constant Heat Source in Nanofluids", *Procedia Eng.*, 127: 978-985.
53. Das S., Jana R. N., Makinde O. D., (2014). "MHD boundary layer slip flow and heat transfer of nanofluid past a vertical stretching sheet with non-uniform heat generation/ absorption", *Int. J. Nanoscience*, 13: 1450019.
54. Bhargava R., Goyal M., Pratibha, (2015). "An efficient hybrid approach for simulating MHD nanofluid flow over a permeable stretching sheet", *Springer Proc. Math. Stat.*, 143: 701-714.
55. Ibrahim W., Shankar B., (2013). "MHD boundary layer flow and heat transfer of a nanofluid past a permeable stretching sheet with velocity, thermal and solutal slip boundary conditions", *Comput. & Fluids*, 75: 1-10.
56. Rashidi M. M., Freidoonimehr N., Hosseini A., Bég O. A., Hung T. K., (2014). "Homotopy simulation of nanofluid dynamics from a non-linearly stretching isothermal permeable sheet with transpiration", *Meccanica*, 49: 469-482.
57. Hamad M. A. A., Ferdows M., (2012). "Similarity solution of boundary layer stagnation-point flow towards a heated porous stretching sheet saturated with a nanofluid with heat absorption/generation and suction/blowing: A Lie group analysis", *Commun. Nonlinear Sci. Numer. Simul.*, 17: 132-140.
58. Sultana T., Saha S., Mansur Rahman Md. M., Saha G., (2009). "Heat transfer in a porous medium over a stretching surface with internal heat generation and suction or injection in the presence of radiation", *J. Mech. Eng.* 40.
59. Mabood F., Khan W. A., Ismail A. I. M., (2015). "MHD Boundary layer flow and heat transfer of nano-fluids over an non- linear stretching sheet: A numerical study", *J. Magn. Magn. Mater.*, 374: 569-576.
60. Khan W. A., Pop I., (2010). "Boundary layer flow of a nanofluid past a stretching sheet", *Int. J. Heat Mass Transf.*, 53: 2477-2483.
61. Goyal, M., Rama Bhargava, (2014). "Boundary layer flow and heat transfer of viscoelastic nanofluids past a stretching sheet with partial slip conditions", *Appl. Nanosci.*, 4: 761-767.
62. Ishak A., Nazar R., Pop I., (2008). "Hydromagnetic flow and heat transfer adjacent to a stretching vertical sheet", *Heat Mass Transf.*, 44: 921-927.
63. Hamad M. A. A., Mahny K. L., Abdel-Salam M. R., (2011). "Similarity Solution of Viscous Flow and Heat Transfer of Nanofluid over a Nonlinearly Stretching Sheet", *Middle-East J. Sci. Res.*, 8: 764-768.
64. Zaimi K., Ishak A., Pop I., (2014). "Boundary layer flow and heat transfer over a nonlinearly permeable stretching/ shrinking sheet in a nanofluid", *Sci. Rep.*, 4: 4404.
65. Rana P., Bhargava R., (2012). "Flow and heat transfer of a nanofluid over a nonlinearly stretching sheet: A numerical study", *Commun. Nonlinear Sci. Numer. Simul.*, 17: 212-226.
66. Malvandi A., Hedayati F., Nobari M. R. H., (2014). "An Analytical Study on Boundary Layer Flow and Heat Transfer of Nanofluid Induced by a Non-Linearly Stretching Sheet", *J. Appl. Fluid Mech.*, 7: 375-384.